

Effect of Friction Stir Welding Parameters on Strength and Fracture Toughness of Dissimilar 6061-2024 Al Joints

Abstract

With increased requirements for high performance on engineering structures in different applications, there is demand for not only new materials but also efficient dissimilar joints being able of providing high-integrity joints. The need to join dissimilar aluminum alloys, such as Al 6061 to Al 2024, is common in many industries and applications. Friction Stir Welding (FSW) has emerged as a promising welding method for joining aluminum alloys, especially dissimilar ones, with the ability to make a joint with superior mechanical properties. However, for this purpose, there is still a shortage of optimum parameters to make a defect-free joint and thus better mechanical properties. In this study, effective dissimilar joints of Al 6061 and Al 2024 with 6 mm thickness were obtained employing FSW with 4 rotational and 3 traverse speeds. The main aim was to achieve the best mechanical performance including fracture toughness. Evaluation of microstructural features, microhardness, tensile, and fracture toughness showed that a good mixture of base metals can result in perfect properties, while an insufficient mixture allows undesirable defects like the void to be created and weaken the properties. Also, the precipitates demonstrated a profound effect on the mechanical behaviors of the samples. The best performance was represented by the rotational speed of 1250 rpm and the traverse speed of 35 mm/min.

Keywords: Friction Stir Welding, Dissimilar Joints, Fracture Toughness, Aluminum, Tensile

1. Introduction

Some properties of aluminum alloys like their low density along with good strength, great corrosion resistance, excellent ductility, proper workability, low electrical resistance, and recyclability have made them a preferential candidate for various applications [1]. There are a great number of applications, however, in which aluminum weldments are made from alloys of different compositional groups. The same is true of a cryogenic situation, a corrosive environment, a high-temperature condition, or other applications in which different performances are essential from different parts of the weldment. Welding dissimilar alloys presents challenges that could lead to issues with weld quality and mechanical properties, therefore it is crucial to select the right process and appropriate parameters to help ensure a prosperous joint. The challenges faced in dissimilar joints are obviously less severe in solid-state welding methods compared to the fusion techniques [2].

Friction Stir Welding (FSW) which at first was designed for aluminum alloys gave a rise to many of these problems and caused huge industrial applicability for aluminum, from aerospace, nuclear, robotics, etc. to less important ones such as general fabrication [2]. This welding process which is capable of producing superior mechanical properties is conducted in solid-state, without melting [3]. FSW is a potential welding process that is used for the joining of similar or dissimilar materials. Compared to other welding techniques, this method represents great advantages. For instance, there is no need of further preparation on the edge pieces or any need for consumables, the process can be automatically and in all positions be accomplished even for those alloys that cannot be traditionally welded, and is environmentally friendly due to its low energy use [3].

However, the consequence of improper FSW parameters is the formation of undesirable defects which cause a lot of problems[4]. Therefore, in all welding cases, the improvement of defect-free, well quality welds is of great importance. As was mentioned earlier, FSW was at first implemented for aluminum and its alloys. Due to that, in recent two decades, optimum parameters for achieving defect-free welds with proper mechanical properties have been found for different types of aluminum alloys in thickness range of less than 1mm to more than 35 mm, even for those that were earlier believed to be infeasible to weld. For example, Moshwan et al. [5] explored the influence of rotational speed with constant traverse speed in FSW on the microstructure and mechanical properties of 5052 aluminum alloy. The rotational speeds were altered from 800 to 3000 rpm and the results revealed that the best tensile properties can be achieved with the rotational speed of 1000 rpm. In another work

conducted by Liu et al.[6], the optimum FSW welding parameters for joining 2017-T351 aluminum alloy were investigated. The experimental results displayed that the tensile properties and fracture locations of the welds are highly affected by the welding parameters. When the revolutionary pitch is larger than a certain value, some voids form in the weld, the tensile characteristics of the welds are significantly low, and the samples are fractured at the center of the weld. Oppositely, when the revolutionary pitch is lesser than the certain value, no voids are made in the welds, the tensile properties of the samples are at quite high levels, and the samples are fractured near or at the interface among the weld nugget and the Thermo-Mechanically Affected Zone (TMAZ). Under the circumstance of an optimum revolutionary pitch of 0.07 mm/rev, the ultimate strength of the joint becomes maximum (82% that of the base material).

Recently, the dissimilar welding of materials especially aluminum alloys has become a popular issue because it provides an insight into too many phenomena that were not obvious among FSW of similar aluminum alloys. Therefore, there have been a lot of efforts to recognize the influence of FSW welding parameters on material flow behavior, and mechanical properties of dissimilar aluminum joints. The effect of some input variables such as tool geometry, rotational and traverse speed, tool plunge depth, and pin offset on joint properties is a challenging topic for researchers. Khan et al. [7] examined two FSW parameters of tool pin offset and tool plunge depth on the formation of defects such as tunnel and kissing bond during welding of dissimilar aluminum alloys of AA5083-H116 and AA6063-T6. The results showed that the tunneling defects existed at all offset and the cross-section of the tunnel varied with the value of offset and the kissing bonds created at the interface for all amounts of pin offset but 0.5 mm. Khodir and Shibayanagi [8] examined the influence of FSW parameters on dissimilar welding of two types of 2024-T3 and 7075-T6 aluminum alloys with two perspectives; "microstructure, and mechanical studies" and "studying of defects including the creation of kissing bond" and they concluded that a rise in traverse speed results in the creation of kissing bonds and pores. Meghnath and co-workers [4] joined two dissimilar aluminum alloys of 5086 and 6061 with FSW in nine experiments with different parameters of tool rotational speed, welding speed and offset of the tool at three levels. Eventually, they successfully found optimum parameters in respect of tensile strength, with the help of statistical optimization tool.

The purpose of this work is to find optimum rotating speed and traverse speed parameters for FSW of two important 6061 and 2024 dissimilar aluminum alloys. The quality of joints is evaluated by fracture toughness, tensile test, hardness, and microscopic observations.

2. Experimental Procedure

In this study, thin plates of Al 2024 and Al 6061-T4 were used as the base metals and their chemical composition and mechanical properties are listed in Tables 1 and 2, respectively. Workpieces with 6 mm thickness, 150 mm length, and 70 mm wide were cut out of the plates and joined with a conventional milling machine with a tool made of H13 material. Tool's geometrical design was composed of a concave shoulder with a 21 mm diameter and a partial cone shape pin with diameters of 7 and 4 mm and a length of 6 mm. Input parameters of tool tilt angle and plunge depth kept to be 2°, and 0.2 mm, respectively. The tool's offset from the weld centerline was set to be 2 mm toward the 2024 plates. In order to investigate the effect of tool rotational and transverse speeds on mechanical properties, 12 different samples with various rotational and transverse speed parameters were prepared as represented in Table 3.

Table 1. Elemental chemical composition of Al 2024-T3 and Al 6061-T4.

Elem ent	Cu	Fe	M g	M n	Si	Zn	Cr	Ti	Al
Al 2024	4. 45	0. 29	1. 53	0. 72	0. 11	0. 12	<0. 01	0. 01	Ba 1.
Al 6061	0. 32	0. 17	1. 08	0. 52	0. 63	0. 2	0.1 02	0. 02	Ba 1.

Table 2. Mechanical Properties of Al 2024-T3 and Al 6061-T4.

Mechanical properties	Yield Strength, MPa	Ultima te Streng th, MPa	Elongatio n, %	Hardness , HV
Al 2024	324	429	18	168
Al 6061	110	211	12	120

Table 3. Welding parameters

Sample No.	Rotational Speed, rpm	Traverse Speed, mm/min
1		35
2	630	65
3		135
4		35
5	800	65
6		135
7		35
8	1000	65
9		135
10		35
11	1250	65
12		135

In order to perform the microscopic survey, the joints were cut and mounted. Then the transverse cross-sections were grinded with the sandpapers from 400 to 3000 grit and polished with the diamond

pastes. After that, they etched with Keller solution (the volume ratio of hydrochloric acid, hydrofluoric acid, nitric acid, and water was 1:1.5:2.5:95). An optical Microscope (OM; Dino Eye. AM 423X) was used to characterize the microstructure of the samples.

In order to do the tensile test, tensile specimens with a width of 12.5 mm and a gauge length of 25 mm were prepared with wire-electrode cutting according to ASTM E8, and the direction of specimens was perpendicular to the weld line. The test was conducted via a tensile testing machine at the test speed of 2 mm/min. After that, the fracture surfaces of specimens were observed using Scanning Electron Microscope (SEM; CAMBRIDGE S-360). In order to perform fracture toughness test, the related specimens which their shape and size were based on ASTM E399, were prepared by wire cutting of welded joints, and then were pre-cracked from the wire cut notch with a load ratio of 0.5 (Fig.1). The test was performed using a uniaxial testing machine with a maximum tensile force of 250 kN.

The microhardness examination has been performed on the surfaces across the joint with the help of KOOPA-MH1 micro hardness machine with 0.1 kg and 20 s dwell time.

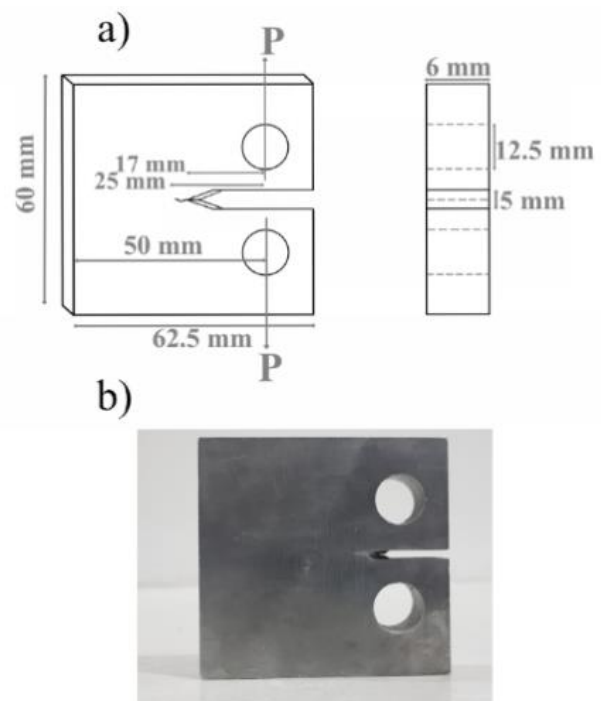


Figure 1. Fracture toughness specimen a) the schematic following ASTM E399 standard, b) the prepared sample.

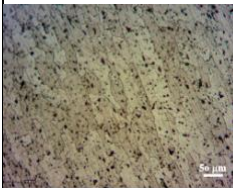
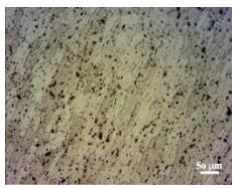
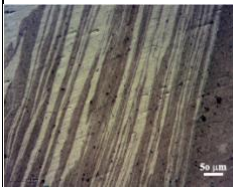
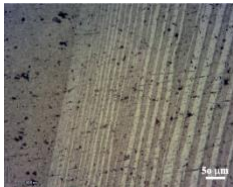
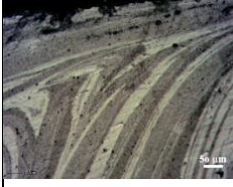

3. Results and Discussion

3.1. Microstructure and Microhardness

Microstructural evolution in the FSW procedure strongly depends on the strain and the temperature tolerated by welded materials [9]. Indeed, the plastic deformation and the heat generated among stirring lead to microstructural changes in nugget and neighboring areas. Generally, the microstructure of FSW joints can be categorized into four zones; I) Stir Zone (SZ) recognized by the region of severely deformed material, II) Thermo-Mechanically Affected Zone (TMAZ) formed by the heating and the deformation caused by tool rotation, III) Heat Affected Zone (HAZ) created due to the thermal cycles of welding, and IV) Base Metal (BM) that is not affected by welding.

Table.4 shows the transfer of material at different locations in samples 10 and 3, with the highest and lowest strength and hardness values, respectively. The shape of mixtures is in agreement with the fact that the matter rotates around the tool before its exit. Also, as it was not far from expectation, the SZ micrograph of sample 10 demonstrates a higher rotational speed compared to sample 2 since its mixture is more uniform. However, it is worth mentioning that even though the picture indicates the final material mixtures, it is not capable of determining the exact materials movement during welding since the material flow is complex and depends on various parameters, including the procedure parameters, tool geometry, and the materials.

Table 4. The shape of different zones in the current study for the samples 10 and 2.

	Sample 10	Sample 3
BM (6061)		
HAZ and TMAZ		
SZ		

For the age hardenable alloys like the ones used in this study, a broad evolving microstructure, especially the precipitate evolution can be produced in the FSW process [10]. The precipitate evolution could lead to big changes in the mechanical properties of the welds as shown on the microhardness distribution maps in Fig. 2. It can be seen that in the microhardness profile of all samples HAZ has the lowest microhardness. Precipitate coarsening or dissolving in the HAZ can be the reason for this phenomenon. Also, the SZ has the highest microhardness, after the 2024 parent metal. The reason lies on the fact that the thermal peak exists in this region, and this high temperature leads to the dissolution of pre-existing precipitants, besides the impossibility of developing new precipitants as a result of the large cooling rate [9]. This observation is in agreement with the findings of M. Paidar et. al. [11]. They employed a modified friction stir clinching of 2024-T3 to 6061-T6 aluminium alloys and found that maximum hardness values were obtained at the centers of the as-welded, and heat-treated samples. Also, they observed that the least microhardness values are obtained at the neighborhood of the TMAZ in both weld groups because of the coarse microstructures. Therefore, the hardness of SZ is a function of particle size and the absence of precipitates in the grains, not a function of grain structure. Moreover, besides the microstructure evolution that occurred through the FSW procedure, natural aging also happens in the weld which is mainly visible in the SZ and affects the betterment of microhardness in this region after a long time [12]. However, further studies, which take advanced electron microscopy techniques into account, will need to be performed to accurately confirm this discusses. It is clear from Fig. 2 that in the constant tool rotational speed, the increase of traverse speed has resulted in the reduction of HAZ distance because of lower temperature increase and decreased of SZ. On the other hand, for the constant traverse speed, the increase of rotational speed made the HAZ distance bigger and the SZ increased because of dynamic recrystallization. Also, the hardness of TMAZ and BM were not influenced by the variation of traverse and rotational speeds. According to the Fig. 2, it can be conducted that the effect of tool rotational speed on the enhancement of hardness is more significant than the traverse speed. Sample 10 demonstrates the best microhardness behavior, with the highest hardness of 137 HV in the SZ and the lowest hardness of 76 HV in the HAZ. The hardness of SZ in this sample is approximately 14% higher than the hardness of weaker base metal (Al 6061).

3.2. Tensile Behavior

Figures 3 and 4 represent the stress-strain curves and ultimate strength of samples, respectively.

Generally, the tensile properties of the samples, to a large extent, depend on their defects and hardness profiles. At lower rotational speeds and higher traverse speeds, the weld cannot obtain enough energy to produce sufficient mixing and be settled in a thermoplastic state. Therefore, it favors voids and other defects to be created in such samples. In this condition, the tensile properties of samples extremely degrade and they face an early fracture. The low elongation of samples 1, 2, 4, and 5 in Fig. 5 is in agreement with this fact. On the other hand, when the mentioned speeds are proper, a defect-free joint can be produced. On this occasion, the tensile properties are a function of hardness distribution [13, 14]. As it was mentioned earlier, the hardness in the weld and the HAZ is lower than the base metals, and this is why the tensile strength of all samples is found to be lower than that of the base materials (Fig. 4). Another reason for this phenomenon can be associated with the reformation of microstructure in the weld zone. Due to the friction and generation of heat through the process, a coarse grain structure is produced which causes lower tensile strength [15]. The results of Figures 3 and 4 show that the best mechanical behavior is represented by sample 10 with an ultimate strength of 207 MPa and elongation of 15.45%, which respectively are about 98% and 129% of those of the weaker alloy 6061. The findings of these two figures also show that for a constant rotational speed, increasing the traverse speed results in the reduction of strength owing to the decrement of hardness value. However, as the rotational speed increases, the effect of traverse speed on strength decreases. For instance, the difference between the ultimate strength of samples having a traverse speed of 135 mm/min and 35 mm/min in rotational speeds of 630 and 1250 was about 220% and 18%, respectively. On the other hand, for a constant traverse speed, the increase of rotational speed increases strength as well. The reason is that the higher rotational speed produces more friction between the base materials and the tool, so plastic deformation occurs more severely, and consequently, more proper bonding in the weld is formed. From Fig. 6 can be concluded that, except for those samples that the defects were their failure reason, the elongation value of specimens regardless of the process parameters were not far from each other. It was anticipated that the weakness of HAZ causes an early fracture and lower elongation value in samples, but interestingly the elongation values of joints were close to that of the base materials. The maximum elongation among all samples is equivalent to 125% of that of the weaker base material. The grain refinement could have been the reason of elongation improvement.

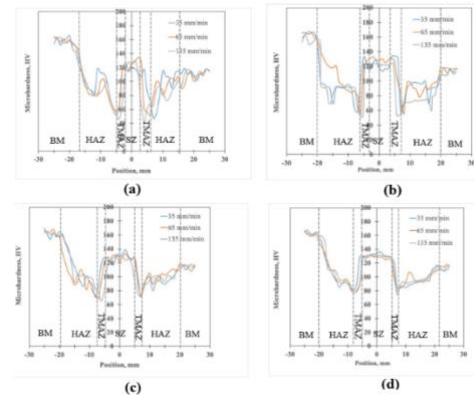


Figure 2. Microhardness profile of samples at different traverse speeds and rotational speeds of a) 630, b) 800, c) 1000, and d) 1250 rpm.

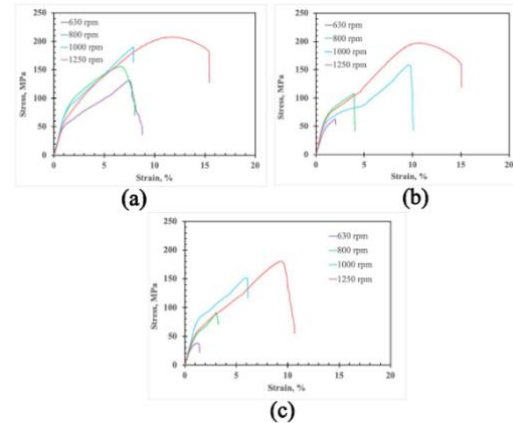


Figure 3. The stress-strain curves of samples at different rotational speeds and traverse speeds of a) 35, b) 65, and c) 135 mm/min

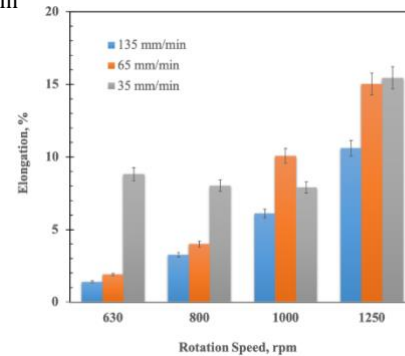


Figure 4. The ultimate strength of samples.

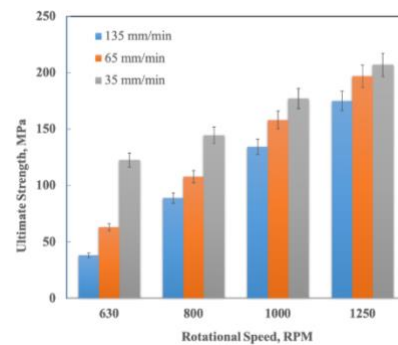


Figure 5. The elongation of samples.

3.3. Fracture Toughness

Generally, fracture toughness is not considered as a problem in aluminum alloys. However, for some certain applications, especially in low-temperature environments, this property is considered to be necessary. Fig.6 represents the fracture toughness values of all joints and Table 5 shows the fracture toughness properties of the two with the highest and the lowest values of them, besides the base materials.

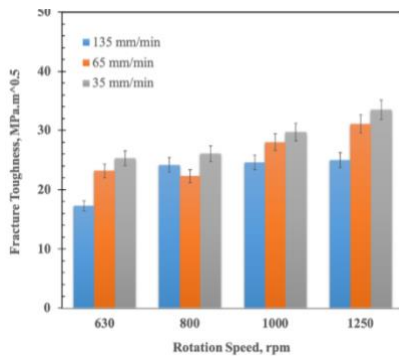


Figure 6. The fracture toughness value of samples.

It can be observed that the fracture toughness of all samples is lower than the stronger base metal in a range between 46.7% and 90.5% of that. The distribution and population of precipitants are the controlling factors for the fracture toughness values. Derry and Robson [16] studied the influence of FSW procedure on the toughness of Al 6013-T6 aluminum alloys. They found that the controlling factors for the toughness in such samples are the population and distribution of the coarse α - (Al, Fe, Si, Mn) intermetallic particles. The absence of precipitants in the SZ and the presence of coarse intermetallic particles in base metals can be the reason for such difference since the precipitates can act as a barrier for the crack growth and therefore, their absence can result in the reduction of fracture toughness values [17, 18]. By increasing rotational speed and/or decreasing traverse speed the fracture toughness rose gradually. The best fracture toughness belongs to sample 10 with above 90% efficiency. The superior mechanical properties of this sample such as its high ultimate strength, and considerable microhardness are the key reasons for this behavior. On the other hand, sample 3 shows the lowest fracture toughness properties. The probability of defects in this sample behaved like a notch which increases the stress intensity factor locally. As a result, fracture happened at the lower P_Q .

Table 5. The fracture toughness properties of base metals and four of the samples.

	P_Q (KN)	P_{max} (KN)	K_Q $MPa.m^{0.5}$	K_{K1C} $MPa.m^{0.5}$
Al6061	5.6	5.7	27.2	27.2
Al2024	7.5	7.9	37.0	37.0
Sample 10	6.6	7	33.5	33.5
Sample 11	6.3	6.5	31.1	31.1
Sample 5	4.5	4.8	22.3	22.3
Sample 3	3.4	3.6	17.3	17.3

3.4. Fractography

It is well known that a joint's fracture location is a clear reflection of its weakest part. It was observed that most of the specimens were fractured at the weld interface and HAZ, which was previously proved that is the weakest region of the weld since it has the lowest hardness values. Fig. 7 shows the SEM images of typical fractured surfaces after tensile and fracture toughness tests. The presence of uniaxial and elongated dimples in Figures 7. a and 7. b (for the tensile test), and 8. c (for the fracture toughness test) reveals the occurrence of ductile fracture. A large number of relatively fine and deep dimples with high plastic deformation on the fracture surfaces is attributed to the fine grain structure in the weld zone which can be the reason for higher elongation and fracture toughness of the related samples. This observation also indicates that the dominant fracture mechanism included the formation, growth, and coalescence of micro-voids [16]. In addition, some of the samples were fractured due to the defects which have formed because of the low material movement. A typical initiated crack by imperfections is detected in Fig. 7.d. Such imperfections can be avoided by setting proper process parameters.

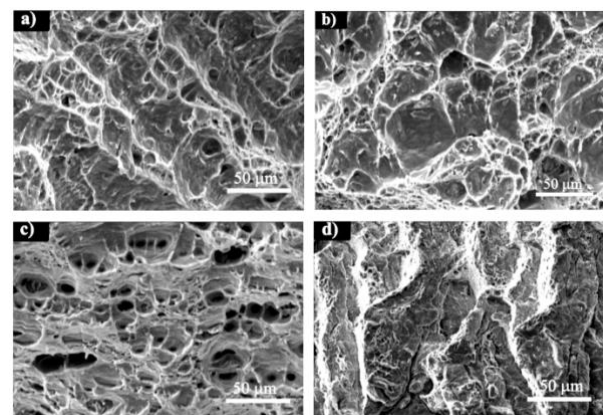


Figure 7. SEM of fractured surfaces after a) tensile test, b) tensile test, c) fracture toughness test, and d) tensile test.

4. Conclusions

In the current study, aluminum alloys of Al 6061-T4 and Al 2024-T3 were successfully friction stir welded together under the following range of parameters: traverse speed of 35-135 mm/min, and rotational speed of 630-1250 rpm. The results below can be concluded from the outcomes of this study:

* In all specimens, the increase of rotational speed and/ or decrease of traverse speed improves the mechanical behavior of weldments, due to the higher heat generation and material flow.

* In the microhardness profiles of samples, HAZ showed the lowest hardness due to grain coarsening. Contradictorily, SZ represented the highest hardness owing to grain refinement and dissolution of precipitates.

* Tensile properties of joins were highly controlled by the microstructure. The samples having defects and insufficient material mixing faced an early fracture and low elongation. While those which had a better mixing demonstrated good tensile behavior with incredible elongation.

* As the precipitates act like a barrier for the crack growth, their absence in the SZ caused lower fracture toughness in all samples compared to the stronger base metal which has coarse intermetallic particles. However, by increasing rotational and/or decreasing traverse speeds the fracture toughness values of samples become closer to the stronger base metal due to the betterment of their mechanical properties.

References

- [1] Stojanović, B., Ivanović, L., 2015. "Application of aluminium hybrid composites in automotive industry". *Tehnički Vjesnik*, 22, 247–251
- [2] Sato, Y.S., Sugiura, Y., Shoji, Y., Park, S.H.C., Kokawa, H., Ikeda, K., 2004. "Post-weld formability of friction stir welded Al alloy 5052". *Materials Science and Engineering A*, 369, 138–143
- [3] Mishra, R.S., Ma, Z.Y., 2005. "Friction stir welding and processing, *Materials Science and Engineering: R: Reports*, 50, 1–78
- [4] Sen, M., Shankar, S., Chattopadhyaya, S., 2019. "Investigations into FSW joints of dissimilar aluminum alloys". *Materials Today: Proceedings*, 27, 2455–2462
- [5] Moshwan, R., Yusof, F., Hassan, M.A., Rahmat, S.M., 2015. "Effect of tool rotational speed on force generation, microstructure and mechanical properties of friction stir welded Al-Mg-Cr-Mn (AA 5052-O) alloy". *Materials and Design*, 66, 118–128
- [6] Liu, H.J., Fujii, H., Maeda, M., Nogi, K., 2003. "Tensile properties and fracture locations of friction-stir-welded joints of 2017-T351 aluminum alloy". *Journal of Materials Processing Technology*, 142, 692–696
- [7] Khan, N.Z., Siddiquee, A.N., Khan, Z.A., Shihab, S.K., 2015. "Investigations on tunneling and kissing bond defects in FSW joints for dissimilar aluminum alloys". *Journal of Alloys and Compounds*, 648, 360–367
- [8] Khodir, S.A., Shibayanagi, T., 2008. "Friction stir welding of dissimilar AA2024 and AA7075 aluminum alloys, *Materials Science and Engineering B: Solid-State*". *Materials for Advanced Technology*, 148, 82–87
- [9] Jacquin, D., Guillemot, G., 2021. "A review of microstructural changes occurring during FSW in aluminium alloys and their modelling". *Journal of Materials Processing Technology*, 288, 116706
- [10] Murr, L.E., 2010. "A Review of FSW Research on Dissimilar Metal and Alloy Systems". *Journal of Materials Engineering and Performance*, 19:8, 19, 1071–1089
- [11] Paidar, M., Tahani, K., Vaira, Vignesh, R., Ojo, O.O., Ezatpour H.R., Moharrami A., 2020. "Modified friction stir clinching of 2024-T3 to 6061-T6 aluminium alloy: Effect of dwell time and precipitation-hardening heat treatment". *Materials Science and Engineering: A*, 791, 139734
- [12] Frigaard, Grong, Midling, O.T., 2001. "A process model for friction stir welding of age hardening aluminum alloys". *Metallurgical and Materials Transactions A*, 32:5, 32, 1189–1200
- [13] Distribution of tensile property and - ProQuest, n.d.
- [14] Liu, H.J., Fujii, H., Maeda, M., Nogi, K., 2003. "Mechanical properties of friction stir welded joints of 1050-H24 aluminium alloy". *Science and Technology of Welding and Joining*, 8, 450–454
- [15] Prabha, K.A., Putha, P.K., Prasad, B.S., 2018. "Effect of Tool Rotational Speed on Mechanical Properties Of Aluminium Alloy 5083 Weldments in Friction Stir Welding". *Materials Today: Proceedings*, 5, 18535–18543
- [16] Derry, C.G., Robson, J.D., 2008. "Characterisation and modelling of toughness in 6013-T6 aerospace aluminium alloy friction stir welds". *Materials Science and Engineering A*, 490, 328–334
- [17] Sivaraj, P., Kanagarajan, D., Balasubramanian, V., 2014. "Fatigue crack growth behaviour of friction stir welded AA7075-T651 aluminium alloy joints". *Transactions of Nonferrous Metals Society of China*, 24, 2459–2467
- [18] Al-Jarrah, J.A., Swalha, S., Mansour, T.A., Ibrahim, M., Al-Rashdan, M., Al-Qahsi, D.A., 2014. "Technical Report". *Materials & Design*, C, 929–936